Journal of Organometallic Chemistry 695 (2010) 1451–1457

Contents lists available at ScienceDirect

Journal of Organometallic Chemistry

journal homepage: www.elsevier.com/locate/jorganchem

Influence of methylimidazole isomers on ferrocene-catalysed nitrogen doped carbon nanotube synthesis

Edward N. Nxumalo [a], Vongani P. Chabalala [a], Vincent O. Nyamori [c], Michael J. Witcomb [b], Neil J. Coville [a,*]

[a] DST/NRF Centre of Excellence in Strong Materials and Molecular Sciences Institute, School of Chemistry, University of the Witwatersrand, Private Bag 3, WITS 2050, South Africa
[b] Microscopy and Microanalysis Unit, and DST/NRF Centre of Excellence in Strong Materials, University of the Witwatersrand, Private Bag 3, WITS 2050, South Africa
[c] The School of Chemistry, University of KwaZulu-Natal, Durban Centre, Private Bag X54001, Durban 4000, South Africa

ARTICLE INFO

Article history:
Received 4 December 2009
Received in revised form 12 February 2010
Accepted 25 February 2010
Available online 3 March 2010

Keywords:
Nitrogen doped carbon nanotubes
Shaped carbon nanomaterials
Bamboo compartment
Ferrocene
Methylimidazoles

ABSTRACT

Nitrogen doped multi-walled carbon nanotubes (N-CNTs) were synthesized by the solid state pyrolysis of ferrocenylmethylimidazole or a mixture of ferrocene (FcH)/*i*-methylimidazole (*i* = 1, 2 and 4) at 800 °C at different ratios in sealed quartz tubes. Transmission electron microscopy (TEM) images confirmed that the carbon nanotubes (CNTs) obtained were doped with nitrogen to give nitrogen doped multi-walled CNTs (N-CNTs). N-CNTs showed bamboo-like structures for the CNTs produced from both ferrocenylmethylimidazole and the mixtures of FcH/*i*-methylimidazole at varying ratios. The study revealed that the different imidazoles produced different types/size distributions of shaped carbon nanomaterials (SCNMs) including N-CNTs with different diameters. An investigation of the bamboo structures revealed that the three methylimidazole isomers led to tubes with different individual bamboo compartment distances and different morphologies including different N contents. This confirms that the synthesis of N-CNTs is determined by fragments (ratios, types) produced by decomposition of reactants at high temperature.

1. Introduction

Since the report on the synthesis of carbon nanotubes (CNTs) in 1991 by Iijima [1], many researchers have devoted much time and effort in developing new strategies for the synthesis of shaped carbon nanomaterials (SCNMs). Organometallic complexes have often been used in the synthesis of these SCNMs that include CNTs [2], carbon nanofibres (CNFs) [3], carbon nanospheres (CNSs) [4], carbon nanocoils [5], etc. The advantages of using organometallic compounds are that they do not need to have a counterion, they do not have to be used in the presence of a support and they act as both a catalyst and as a carbon source to form SCNMs. Initial reports using organometallic complexes such as ferrocene [6], cobaltocene [7] and nickelocene [8], under reducing conditions revealed that the pyrolysis of the metallocenes generated CNTs.

When ferrocene is used together with a carbon source, the Fe/C ratio has a major impact on whether CNTs or CNSs are the major products formed in the reaction [9]. Low catalyst concentrations favour CNT production and the absence of a catalyst leads only to CNSs and amorphous materials [10]. Increasing the Fe/C ratio leads to an increase in the diameter of the nanotubes produced due to the formation of larger iron nanoparticles at higher metal concentration [9]. An increased Fe/C ratio also leads to a higher yield of iron filled CNTs [9a].

Doping of CNTs with heteroatoms leads to a change in the CNT structure. Nitrogen, for example, has profound effects on the nanotube morphology [11,12]. The presence of nitrogen in the growth environment is a favourable condition for the formation of 'bamboo-like' CNTs, but it is not a necessary condition [13–15]. N-doping of CNTs can be achieved by *in situ* N addition during CNT formation or post-synthesis doping of undoped CNTs. The doping of CNTs has been reported previously [16]. The routine method for the *in situ* synthesis of nitrogen doped CNTs (N-CNTs) is the chemical vapour deposition (CVD) method using nitrogen containing compounds [17]. Ammonia [18] or any volatile nitrogen-compound containing an organic component can be used as an N source. Most experiments performed using nitrogen gas or ammonia in a CVD process generate vertically aligned CNTs [19]. Films of vertically grown N-CNTs from different substrates have also been obtained by the pyrolysis of a mixture of ferrocene and melamine [20]. Li et al. [21] have shown that it is possible to grow high quality vertically oriented N-CNT arrays over an alumina substrate on a rough surface. Qian et al. [22] successfully synthesized well-aligned N-doped multi-walled carbon nanotube arrays over a large area, on quartz and silicon wafers, by a floating catalyst CVD method at fairly low temperature (600 °C) using pyridine–ferrocene mixtures. The nitrogen incorporated nanotubes have smaller outer diameters but larger inner diameters compared with CNTs grown from a xylene–ferrocene mixture under similar conditions [22].

N-CNTs have recently shown great potential as catalyst supports for Pt–Ru nanoparticles in the anodic oxidation of methanol in direct methanol fuel cells [23]. They have also been used in

* Corresponding author. Tel.: +27 11 717 6738; fax: +27 11 717 6749.
E-mail address: neil.coville@wits.ac.za (N.J. Coville).

0022-328X/$ - see front matter © 2010 Elsevier B.V. All rights reserved.
doi:10.1016/j.jorganchem.2010.02.028

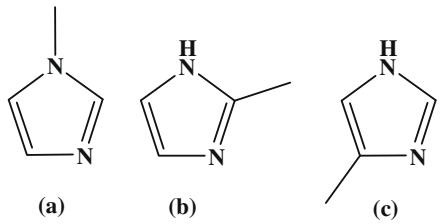

Fig. 1. Structures of the N sources used during the formation of SCNMs: (a) 1-methylimidazole; (b) 2-methylimidazole and (c) 4-methylimidazole.

environmental applications, in the aqueous phase, as adsorbents of organic and inorganic compounds and ions [24]. A recent review described theoretical studies involving carbon nanostructures that have been substitutionally doped with transition metals and nitrogen atoms [12]. Literature reports reveal that the incorporation of N into CNTs results in an enhancement in conductivity [25] and improvement of transport and field emission properties of CNTs [26]. N-doped single-walled CNTs (SWCNTs) synthesized in large scale using an electric arc discharge method show that the band gap of SWCNTs can be tuned by varying the degree of N insertion [27]. This is due to the electron donor ability of the nitrogen atom that leads to the formation of a n-type semiconductor [28].

More recently there has been an upsurge of interest in the synthesis of CNTs by the pyrolysis of organometallic complexes in a confined environment e.g. stainless steel autoclaves or sealed glass vessels, at autogenous pressure especially using Fe and Co metal catalysts [29]. Undoped CNTs can be produced in high yields by directly pyrolyzing ferrocene in an autoclave [30]. Zhang et al. [31] also synthesized larger diameter undoped CNTs through the catalytic decomposition of polypropylene and maleated polypropylene using Ni as a catalyst in an autoclave at 700 °C. The possible growth process for CNTs grown using this method was also described.

In this work, we report the N-doping of multi-walled CNTs in a confined space (sealed quartz vessels) using organometallic precursors. The use of ferrocenylmethylimidazole as a catalyst for the synthesis of N-CNTs as well as the use of different ratios of ferrocene/*i*-methylimidazole (*i* = 1, 2 or 4) (Fig. 1) in a confined space yielded N-CNTs with different morphologies and several other SCNMs. Furthermore, we reveal that the growth of N-CNTs is determined by the fragments produced by decomposition of the reactants and that the different imidazoles yield N-CNTs with different nitrogen contents.

2. Experimental

2.1. General procedure

The synthesis of ferrocenyl derivatives were performed under an inert atmosphere of pure argon. This was achieved by using standard Schlenk techniques. Silica Gel 60 was used for column chromatography. Commercial dichloromethane was initially dried over calcium chloride, and then distilled from calcium hydride. Preparation of anhydrous diethyl ether was achieved by drying over fresh sodium wire. Ferrocene and ferrocene carboxaldehyde were purchased from Strem Chemicals, Inc. (USA). The three isomers (1-methylimidazole, 2-methylimidazole and 4-methylimidazole) were purchased from Sigma–Aldrich.

2.2. Instrumentation

Raman spectra were measured using the single spectrograph stage of a Jobin–Yvon T64000 Raman spectrometer. The excitation source was 636.4 nm from a tunable Spectra-Physics dye laser. The laser beam was focused onto the sample using the 20× objective of an Olympus microscope. The backscattered light was dispersed using a 600 line/mm grating and detected using a CCD detector. Thermogravimetric analysis (TGA) measurements were performed under air on a Perkin–Elmer TGA 7 at a heating rate of 10 °C/min. TEM analysis was performed on a JEOL JEM-100S Electron Transmission Microscope at 80 kV and on a Philips CM200 (Philips, Eindhoven, The Netherlands) equipped with a Gatan Imaging Filter. The TEM samples were dispersed in methanol using an automated sonicator and loaded onto a holey Cu grid.

2.3. Synthesis of ferrocene derivatives

2.3.1. Synthesis of ferrocenylmethylimidazole

Ferrocenylmethanol was obtained by the reduction of ferrocene carboxylaldehyde using an ethereal solution of lithium aluminium hydride. Ferrocenylmethylimidazole was achieved by reacting equimolar amounts of ferrocenylmethanol and *N,N*-carbonylimidazole in anhydrous dichloromethane in an inert atmosphere [32].

2.3.2. Synthesis of SCNMs in sealed tubes

Approximately 100 mg of precursor compounds (ferrocenylmethyimidazole or FcH/methylimidazole) were sealed in a quartz tube (10 cm in length and 1.0 cm internal diameter). The quartz tube (Fig. 2(a)) was introduced into an electrical furnace and heated at a rate of 3 °C/min to reach a temperature of 500 °C *i.e.* above the precursor decomposition temperature. The tubes were held at this temperature for at least 30 min to ensure complete decomposition of reagents. The tube was then heated at a rate of 2 °C/minute to 800 °C and held at that temperature for 12 h before being gradually cooled to room temperature. A black solid material was obtained (Fig. 2(b)). A small amount of the black carbonaceous material was transferred into a mortar and ground using a pestle to a fine material. The sample was then characterized by TEM, TGA and Raman spectroscopy.

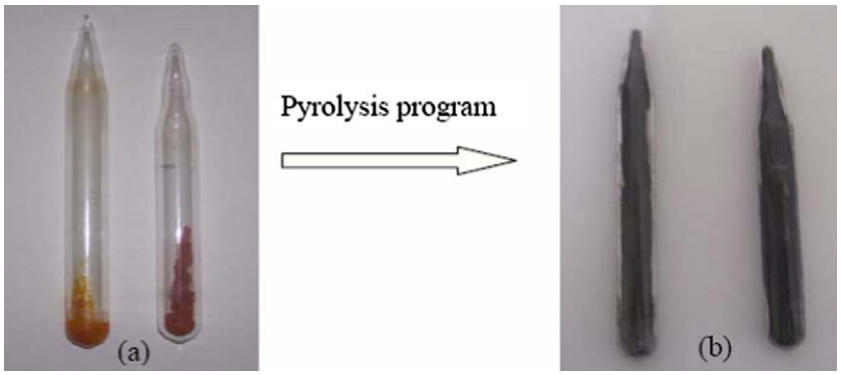

Fig. 2. Quartz tube reaction vessels (a) before and (b) after reaction.

3. Results and discussion

3.1. Synthesis of ferrocenylmethylimidazole

Ferrocenylmethylimidazole was synthesized from equimolar amounts of ferrocenylmethanol and *N,N*-carbonylimidazole in anhydrous dichloromethane as reported by Simenel et al. [32]. The chemical structures of these two compounds were confirmed by ^{1}H NMR, ^{13}C NMR and FTIR spectroscopies and XRD patterns.

3.2. Synthesis of carbon nanotubes

Carbonaceous materials were synthesized successfully by the solid state pyrolysis of ferrocenylmethylimidazole or varying ratios of mixtures of FcH and methylimidazole in sealed quartz tubes. The advantage of this procedure is that the effect of high pressure on product formation can be utilized. Methylimidazoles were chosen for study as they have a high N content (~30% by mass), are air-stable and exist as solids and liquids. Reaction conditions were chosen to ensure breakdown of the reactants by decomposition. In the closed environment the reactants will break down into C, H, N and Fe containing species [33]. The conditions will produce ionic species as well as radicals, molecular species and ions, and the type of reactant and the reactant ratio could thus impact on the products formed.

In this study the effect of the position of the methyl group in methylimidazole has been investigated in the synthesis of nitrogen doped CNTs. In particular, three different methylimidazoles (*i.e.* 1, 2 or 4-methylimidazole) were chosen for investigation. As these compounds all have the same elemental composition any differences in the products formed will relate to the position of the Me group on the ring backbone. In principle, if they all break down completely under the reaction conditions then all three isomers should generate similar ratios and types of carbonaceous products. Indeed the current mechanism proposed for CNT growth involves carbon atoms dissolving in a catalyst and re-precipitating to give CNT growth [34]. The three methylimidazole isomers do, however, have different physical and chemical properties and hence we may expect decomposition products and rates to be different.

In this investigation, the pyrolysis reactions all gave black carbonaceous materials that were then analysed by TEM, TGA and Raman spectroscopy.

3.2.1. TEM analysis of CNTs

TEM analysis was used to evaluate the products generated in the pyrolysis reactions. TEM images showed that different products (amorphous carbon, spheres, fibres, hollow tubes and bamboo tubes) were obtained from the different reactions and the data is summarised in Table 1. All the tubes obtained in this study were of the multi-walled type and TEM images of typical N-CNT products are shown in Figs. 3 and 4. The product morphology distributions were estimated from the TEM photographs and while the error bar was *ca.* 5–10%, trends in the morphologies can still be noted. The product ratios indicate that the type of imidazole used did indeed impact on the product distribution detected.

In these systems there is no flowing H_2 since the reactions are performed in sealed quartz tubes. Thus the formation of amorphous carbon is inevitable [35]. The molecules FcH and ferrocenylmethylimidazole generally give tubes which are cleaner compared to those obtained from the FcH/methylimidazole mixtures (e.g. the 50/50 mix) under analogous reaction conditions. Such an observation is also common for floating catalyst systems [17,36].

While the amorphous carbon and the spheres may have contained nitrogen, it is not possible to determine the nitrogen content in these materials. In contrast, CNTs that contain nitrogen can readily be detected by the bamboo morphology that is characteristic of the Fe catalysed synthesis of N-CNTs [37–39]. Thus analysis of this sub-set of products allows for an analysis of the effect of nitrogen on the CNT products generated.

3.2.2. Effect of FcH/imidazole ratio

The TEM images of CNTs grown from ferrocene (100%) show hollow tubes (outer diameter = 120 nm and inner diameter = 60 nm) that typically contain encapsulated iron nanoparticles (Supplementary material, Fig. S1). The data shows that the products obtained are similar to those obtained in a typical floating catalyst flow system (except for the production of more amorphous material in the closed systems) [40].

The average outer diameters (ODs) of the multi-walled CNTs (MWCNTs) produced from ferrocenylmethylimidazole were 70 nm, whilst their average internal diameters (IDs) were 30 nm. These narrower tubes (relative to FcH) are expected [41]. Importantly, the presence of nitrogen has resulted in the expected formation of bamboo N-CNTs. Images of the bamboo morphology are shown in Fig. 4a.

Of more interest is the impact of the mixtures of FcH and methylimidazoles on the products produced. Remarkably the position of the ring substituent impacts on both the product distribution (in particular N-CNT yield) and the product morphology (N-CNT diameters) (see Table 1). Thus, for a FcH/*i*-methylimidazole

Table 1
Relative% distribution of CNTs, CNFs, CNSs and a-C with the size distribution and the relative yields produced from the pyrolysis of FcH, ferrocenylmethylimidazole and FcH/*i*-methylimidazole at varying ratios.

Catalyst used to grow CNTs	Fe/H ratio	SCNMs (%)	Diameters (nm)	Yield (mg)
FcH (100%)	0.100	80T, 20a-C	120(OD), 60(ID)	78.2
Ferrocenylmethylimidazole (100%)	0.0714	50T, 20F, 30a-C	70(OD), 30(ID)	73.0
FcH/1-methylimidazole (90:10)	0.0833	40T, 60a-C	90(OD), 40(ID)	51.2
FcH/2-methylimidazole (90:10)	0.0833	30T, 5S, 65a-C	150(OD), 120(ID)	67.0
FcH/4-methylimidazole (90:10)	0.0833	30T, 5F, 65a-C	100(OD), 40(ID)	59.1
FcH/1-methylimidazole (80:20)	0.0769	45T, 5S, 50a-C	100 OD, 25 ID	46.1
FcH/2-methylimidazole (80:20)	0.0769	45T, 5F, 55a-C	140 OD, 120 ID	65.9
FcH/4-methylimidazole (80:20)	0.0769	35T, 15F, 50a-C	120 OD, 100 ID	62.5
FcH/1-methylimidazole (50:50)	0.0435	50T, 10F, 40a-C	70(OD), 20(ID)	44.8
FcH/2-methylimidazole (50:50)	0.0435	30T, 10F, 60a-C	60(OD), 25(ID)	47.5
FcH/4-methylimidazole (50:50)	0.0435	5T, 35S, 60a-C	50(OD), 20(ID)	46.1
FcH/1-methylimidazole (20:80)	0.0156	70T, 20F, 10a-C	100 OD, 80 ID	30.7
FcH/2-methylimidazole (20:80)	0.0156	80T, 10F, 10a-C	90 OD, 40 ID	30.0
FcH/4-methylimidazole (20:80)	0.0156	10T, 5F, 85a-C	50 OD, 20 ID	40.4
FcH/1-methylimidazole (10:90)	0.0076	30T, 30F, 40a-C	80(OD), 40(ID)	14.2
FcH/2-methylimidazole (10:90)	0.0076	10T, 40F, 50a-C	70(OD), 40(ID)	37.7
FcH/4-methylimidazole (10:90)	0.0076	5T, 45F, 50a-C	35(OD), 10(ID)	40.2

T = Tubes, F = CNFs, S = CNSs, a-C = amorphous carbon.

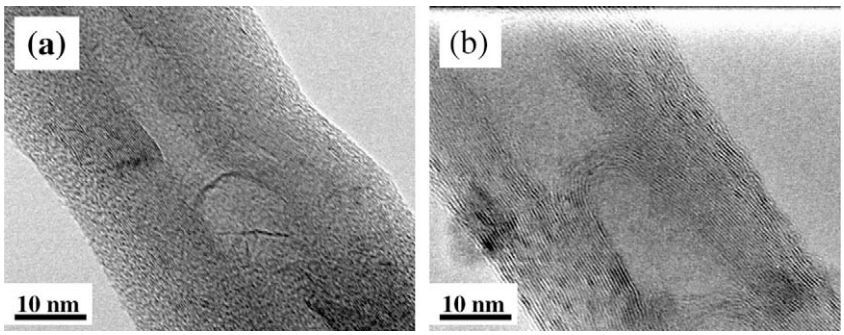

Fig. 3. HRTEM images of N-CNTs grown from the pyrolysis of (a) FcH/4- methylimidazole (50:50) and (b) ferrocenylmethylimidazole.

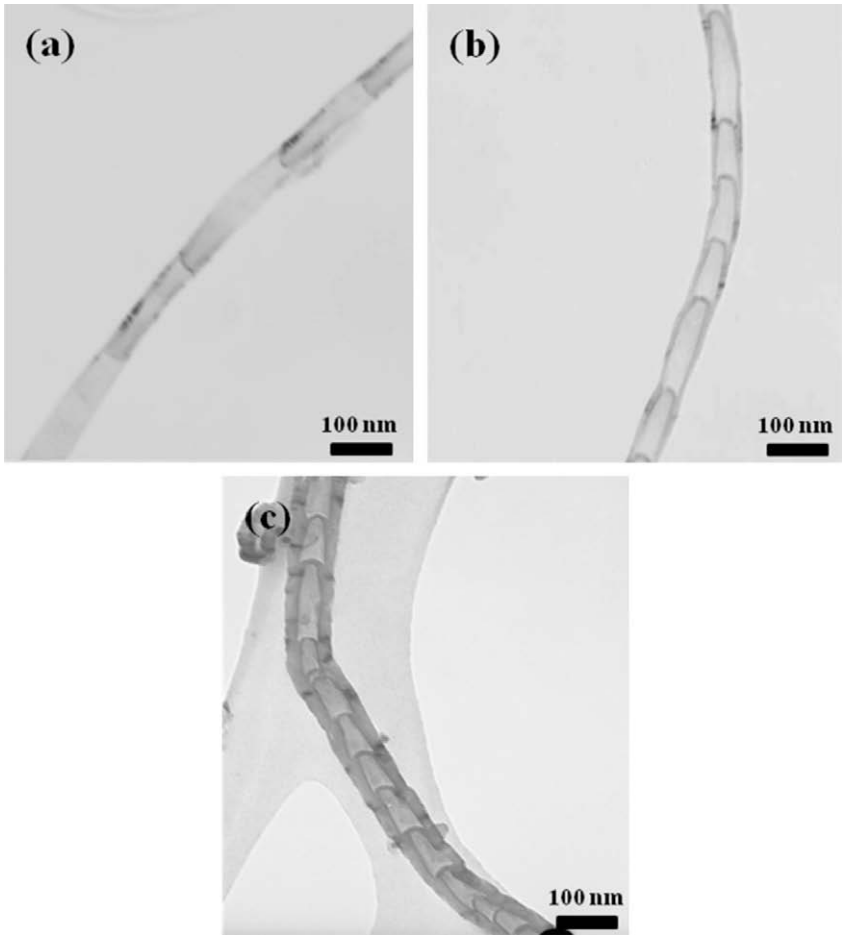

Fig. 4. TEM images of N-CNTs showing bamboo structures grown from the pyrolysis of (a) FcH/1-methylimidazole; (b) FcH/2- methylimidazole and (c) FcH/4-methylimidazole.(50:50).

(50:50) mixture the N-CNT yields decreased in the order $i = 1 > 2 > 4$. Further, the average tube inner and outer diameters generally became smaller, in the order $i = 1 > 2 > 4$. This decrease in diameter suggests a higher degree of N-doping of the CNTs (increase in N concentration) as has been suggested previously [42]. The product data for the FcH/methylimidazole mixture are most similar to the products obtained from ferrocenylmethylimidazole.

The degree of N-doping also could be calculated from the % of the CNTs that had a bamboo structure or an open structure. For examples, the pyrolysis of FcH/1-methylimidazole gave a degree of doping of 15% while FcH/2-methylimidazole gave a degree of doping of 75% at a similar ratio (50:50). FcH/4-methylimidazole (50:50) and ferrocenylmethylimidazole gave higher degrees of doping (>95%). This is consistent with the observed tube diameters as well as the bamboo compartment distances (Figs. 7 and 8).

Other FcH/*i*-methylimidazole ratios were also used to study the reaction (90:10; 80:20; 20:80; 10;90). The *general* trends noted were:

(i) The trends listed above for the 50:50 ratio hold (in general) for the other ratios.
(ii) The total yields of all products decreased with increasing imidazole content.
(iii) Increasing the Fe/C ratio results to an increase in the diameter of the CNTs. This is related to the formation of larger iron nanoparticles when a higher catalyst content is used.

(iv) These higher Fe/H ratios (0.100) favour the formation of more CNTs while at lower Fe/H ratios (0.0076) more amorphous material is generated (see Table 1). This is associated with the formation of more gaseous materials under a more reducing atmosphere.
(v) Most samples contained >10% of Fe filled nanotubes.

The products obtained from the three imidazoles are thus different in terms of yields and morphologies. This could be due to breakdown products produced in the reaction. Clearly the manner in which decomposition occurs varies with the imidazole used. The three imidazoles are structural isomers; hence, they have different physical and chemical properties. The difference in their physical properties should affect the rate and nature of their decomposition.

3.2.3. Analysis of the bamboo structures

In a previous study, we have quantified the N content of CNTs, using XPS and CHN analysis. In this study this is not possible due to the large amount of non-CNT products formed. However the amount of N added to a CNT can be correlated to the distance between individual bamboo compartments [17]. The larger the bamboo compartments the lower the nitrogen content of the N-CNTs produced when similar reaction conditions are used [43].

The N-CNTs produced from the FcH/*i*-imidazole 50:50 mixtures were analysed for their nitrogen content using the procedure described above. The distance between bamboo compartments (Fig. 4) was measured from TEM images (>200 measurements per sample) for each of the imidazole samples produced. The distance between the bamboo 'caps' within a N-CNT is clearly seen to vary with the positioning of the methyl group in the imidazole (Figs. 5 and 6 and Fig. S2 and S3 (Supplementary material)). Tubes grown from 1-methylimidazole have a larger compartment distance (avg value = 210 nm) followed by those obtained from 2-methylimidazole (avg = 95 nm) and those obtained from 4-methylimidazole (avg = 40 nm). These results indicate that the N-CNTs produced from 4-methylimidazole have a higher N content; a result consistent with the tube diameter analysis described above.

The average distance between individual bamboo compartments obtained from the pyrolysis of ferrocenylmethylimidazole was found to be 45 nm, close to the N-CNT values obtained from 4-methylimidazole (Fig. 6). High *N* values are expected for the CNTs produced from ferrocenylmethylimidazole due to the proximity of N group to the Fe catalyst in the reaction [14].

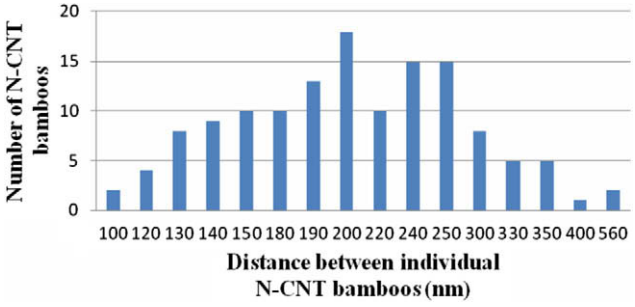

Fig. 5. Distance between individual bamboo compartments obtained from the pyrolysis of 1-methylimidazole (50:50).

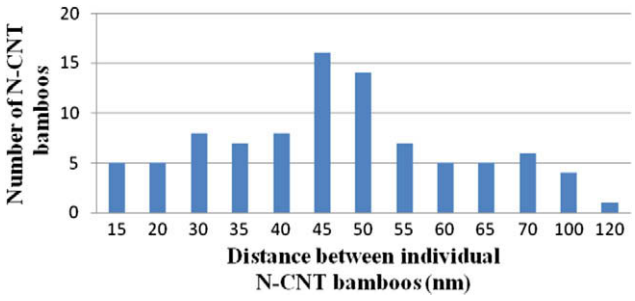

Fig. 6. Distance between individual bamboo compartments obtained from the pyrolysis of ferrocenylimidazole.

3.3. TGA analysis

Thermogravimetric analysis (TGA) of nanotubes under O_2 is a useful technique for studying the thermal stability of carbonaceous samples. The shape of the TGA curve can give information about the presence of carbon by-products, such as amorphous carbon [44,45].

All samples prepared in this study showed similar oxidation behaviour in TGA experiments and typical TGA profiles are shown in Fig. 7. A slight weight loss at ~200 °C is due to the loss of water and organic volatiles. Decomposition of the CNTs was observed from 450 to 610 °C. Generally, this accounts for most of the weight loss (60%). It has been observed that the N-CNTs are generally less stable than the undoped CNTs (prepared from FcH) and hence should decompose at lower temperatures [46]. This is reportedly caused by the presence of a higher defect content in their walls [47]. Most of the tubes have 5–20% residual weight after oxidation (Fig. 7). This is attributed to the metal residue (FeOx) that remains after carbon has been oxidized. This residual weight varies with

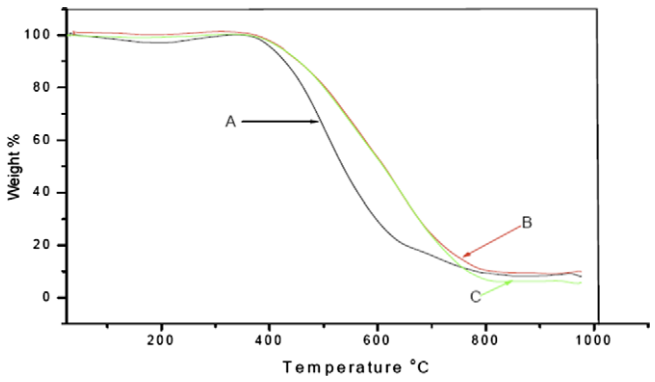

Fig. 7. TGA curves of CNTs grown from (A) FcH/1-methylimidazole (10:90); (B) FcH/2-methylimidazole (10:90) and (C) FcH/4-methylimidazole (10:90).

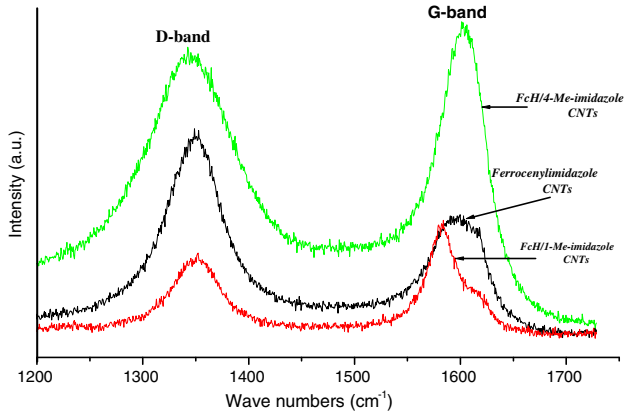

Fig. 8. Raman spectra of CNTs grown from ferrocenylmethylimidazole, FcH/1-methylimidazole (50:50) and FcH/4-methylimidazole (50:50).

the amount of FcH used in the synthesis of the CNTs (Table 1) [48,49]. Of note is the slight weight gain around 400 °C, due to oxidation of the residual Fe catalyst trapped in the tubes.

3.4. Raman analysis

Raman spectroscopy was used to obtain information about disorder in the carbon materials. For most spectra, three peaks are observed: a peak around 1350 cm^{-1} (the D-band), a peak around 1580 cm^{-1} (the G-band) and a small shoulder at around 1615 cm^{-1}. The Raman D-band is associated with disorder and is a manifestation of an in plane vibrational mode. The G-band originates from the symmetric vibrations of the Raman active E_{2g} mode [50]. The small shoulder at around 1615 cm^{-1} is also induced by disorder.

The intensity ratio (I_D/I_G) indicates the degree of disorder of the SCNMs. When samples are compared the I_D/I_G ratio can establish which sample contains the most graphitic (most ordered) structure. Disorder can arise from the range of structures produced as well as the degree of N-doping of the CNTs. The ratios are displayed in the Supplementary material (Table S1). Fig. 8 shows the Raman spectra for samples grown at a similar reactant ratio (50:50). Generally, a dramatic broadening of the D- and G-band is seen in these crude samples (compared with the undoped CNT) [43]. Further, the I_D/I_G ratio of the samples varied with the FcH/imidazole ratio. This observation can be correlated to the products obtained from the three different imidazole isomers. It appears that, in general (and as expected), reactions with 4-methylimidazole give the largest I_D/I_G ratios.

3.5. Mechanism

A mechanism that leads to the formation of N-CNTs with different morphologies generated from the pyrolysis of imidazole isomers can be proposed (Fig. 9). When heated to elevated temperatures, imidazoles decompose to form radicals, ions and molecular species (Fig. 9, step 1). Under suitable conditions these decomposition products will break down further to C and N atoms (step 2), which then interact with Fe nanoparticles to form N-CNTs and other carbon species via the classical CNT growth mechanism [34].

The mechanism above does not however fully account for the different products and product ratios that are formed from the different imidazole isomers and that could lead to the different product yields and morphologies. The three imidazole isomers decompose to give different breakdown products. This is associated with the different physical and chemical properties and different methyl group and C=N positions in the different isomers and that lead to the formation of the different decomposition products. This suggests that the radicals, ions and molecular species formed can interact directly with the Fe nanoparticles (step 4). Presumably these radicals, ions and molecular species then decompose to C and N atoms that eventually lead to the N-CNT growth. This would suggest control (*via* the breakdown products) of CNT morphology by chemical procedures is possible. This proposal indicates that CNT growth can be controlled by the choice of reactants, as has been suggested by others [14,33]. Thus a key finding from our experiments is that control of species formed in the reaction can be controlled by the chemical nature of the reactants. Experiments to further probe the above proposal are currently underway.

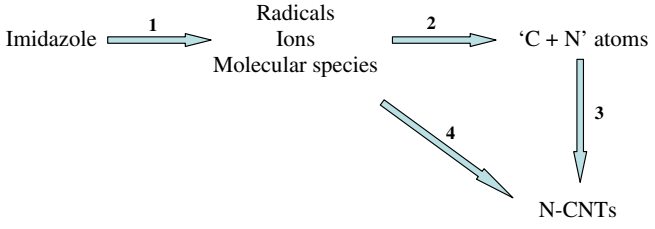

Fig. 9. A model for the formation of N-CNTs from the methylimidazole decomposition.

4. Conclusion

A method for the N-doping of CNTs based on the pyrolysis of ferrocenes and immidazoles in a confined environment has been described. We have shown that the position of the methyl group attached to the imidazole can influence the size distribution and the type of SCNMs produced in the 'autoclave' system. An analysis of the SCNMs and the bamboos structures reveals that the three structural isomers of methylimidazoles lead to different products; in particular with N-CNTs that contain different amounts of N as determined by measurements of bamboo compartments and tube diameters. The results show that the control of N-CNTs is determined by fragments produced by decomposition of reactants at high temperature.

Acknowledgements

The authors wish to thank the DST/NRF Centre of Excellence in Strong Materials and the University of the Witwatersrand for financial support.

Appendix A. Supplementary material

Supplementary data associated with this article can be found, in the online version, at doi:10.1016/j.jorganchem.2010.02.028.

References

[1] S. Iijima, Nature 354 (1991) 56.
[2] (a) A. Govindaraj, C.N.R. Rao Pure, Appl. Chem. 74 (2002) 1571;
(b) R. Sen, A. Govindaraj, C.N.R. Rao, Chem. Phys. Lett. 267 (1997) 276;
(c) C.N.R. Rao, R. Sen, B.C. Satishkumar, A. Govindaraj, Chem. Commun. (1998) 1525.
[3] (a) R. Andrews, D. Jacques, A.M. Rao, F. Derbyshire, D. Qian, X. Fan, E.C. Dickey, J. Chen, Chem. Phys. Lett. 303 (1999) 467;
(b) R. Kamalakaran, M. Terrones, T. Seeger, P. Kohler-Redlich, M. Rühle, Y.A. Kim, M. Endo, Appl. Phys. Lett. 77 (2002) 3385;
(c) A. Cao, L. Ci, G. Wu, B. Wei, C. Xu, J. Liang, D. Wu, Carbon 39 (2001) 152;
(d) E.C. Dickey, C.A. Grimes, M.K. Jain, K.G. Ong, D. Qian, P.D. Kichambare, R. Andrews, D. Jacques, Appl. Phys. Lett. 79 (2001) 4022;
(e) M. Mayne, N. Grobert, M. Terrones, R. Kamalakaran, M. Rühle, H.W. Krato, D.R.M. Walton, Chem. Phys. Lett. 338 (2001) 101.
[4] (a) F. Rohmund, L.K.L. Falk, E.E.B. Campell, Chem. Phys. Lett. 328 (2000) 369;
(b) X.Y. Liu, B.C. Huang, N.J. Coville, Carbon 40 (2002) 2791.
[5] (a) S. Amelinckx, X.B. Zhang, D. Bernaerts, X.F. Zhang, V. Ivanov, J.B. Nagy, Science 265 (1994) 635;
(b) M. Zhang, Y. Nakayama, L. Pan Japan, J. Appl. Phys. 39 (2000) L1242;
(c) L. Pan, T. Hayashida, Y. Nakayama, J. Mater. Res. 17 (2001) 45;
(d) C. Kuzuya, W. Hwang, S. Hirako, Y. Hishikawa, S. Motojima, Chem. Vapor Deposition 8 (2002) 57;
(e) V.K. Varadan, J. Xie, Smart Mater. Struct. 11 (2002) 728.
[6] (a) X. Zhang, A. Cao, B. Wei, Y. Li, J. Wei, C. Xu, Wu D, Chem. Phys. Lett. 362 (2002) 285;
(b) C. Singh, M. Schaffer, I. Kinloch, Physica B 323 (2002) 339;
(c) B. Wei, R. Vajtai, Y.Y. Choi, P.M. Ajayan, Nano Lett. 2 (2002) 1105;
(d) C. Singh, M.S.P. Schaffer, A. H Windle, Carbon 41 (2003) 59.
[7] C. Singh, T. Quest, C.B. Boothroyd, P. Thomas, I.A. Kinloch, A.I. Abou-Kandil, A.H. Windle, J. Phys. Chem. B 106 (2002) 10915.
[8] C.N.R. Rao, A. Govindaraj, Acc. Chem. Res. 35 (2002) 998.
[9] (a) V.O. Nyamori, N.J. Coville, Organomet. 26 (2007) 4083;
(b) M.S. Mohlala, X.-Y. Liu, J.M. Robinson, N.J. Coville, Organomet. 24 (2005) 972;
(c) J. Cheng, X.P. Zou, G. Zhu, M.F. Wang, Y. Su, G.Q. Yang, X.M. Lü, Solid State Commun. 149 (2009) 1619.
[10] S. Bai, F. Li, Q-H. Yang, H-M. Cheng, J-B. Bai, Chem. Phys. Lett. 376 (2003) 83.
[11] (a) M. Terrones, P.M. Ajayan, F. Banhart, X. Blase, D.L. Carroll, J.C. Charlier, et al., Appl. Phys. A 74 (2002) 355;
(b) P. Redlich, J. Loeffler, P.M. Ajayan, J. Bill, F. Aldinger, M. Rühle, Chem. Phys. Lett. 260 (1996) 465;

(c) Z. Weng-Sieh, K. Cherrey, N.G. Chopra, X. Blase, et al., Phys Rev. 51 (1995) 11229.
[12] J.W. Jang, C.E. Lee, S.C. Lyu, T.J. Lee, C.J. Lee, Appl. Phys. Lett. 84 (2004) 2877.
[13] C.H. Lin, H.L. Chang, C.M. Hsu, A.Y. Lo, C.T. Kuo, Diamond Relat. Mater. 12 (2003) 1851.
[14] M. Jung, K.Y. Eun, J.-K. Lee, Y.-J. Baik, K.-R. Lee, J.W. Park, Diamond Relat. Mater. 10 (2001) 1235.
[15] L.M. Cao, X.Y. Zhang, C.X. Gao, W.K. Wang, Z.L. Zhang, Z. Zhang, Nanotechnology 14 (2003) 931.
[16] (a) R. Sen, B.C. Satishkumar, A. Govindaraj, K.R. Harikumar, M.K. Renganathan, C.N. R Rao, J. Mater. Chem. 7 (1997) 2335;
(b) R. Sen, B.C. Satishkumar, A. Govindaraj, K.R. Harikumar, G. Raina, J.-P. Zhang, A.K. Cheetham, C.N. R Rao, Chem. Phys. Lett. 287 (1998) 671;
(c) M. Nath, B.C. Satishkumar, A. Govindaraj, C.P. Vinod, C.N.R. Rao, Chem. Phys. Lett. 322 (2000) 333;
(d) L.S. Panchakarla, A. Govindaraj, C.N.R. Rao, ACS Nano 1 (2007) 494.
[17] (a) E.N. Nxumalo, V.O. Nyamori, N.J. Coville, J. Organomet. Chem. 693 (2008) 2942;
(b) T.-Y. Kim, K.-R. Lee, K.Y. Eun, K.-H. Oh, Chem. Phys. Lett. 372 (2003) 603.
[18] C.J. Lee, S.C. Lyu, H-W. Kim, J.H. Lee, K.L. Cho, Chem. Phys. Lett. 359 (2002) 115.
[19] (a) N.H. Quang, M.V. Trinh, B-H. Lee, J-S. Huh, Sens. Actuators, B 113 (2006) 341;
(b) C. Tang, Y. Bando, T. Sato, Chem. Phys. Lett. 362 (2002) 185.
[20] Y. Chai, Q.F. Zhang, J.L. Wu, Carbon 44 (2006) 687.
[21] Y.-L. Li, F. Hou, Z.-T. Yang, J.-M. Feng, X.-H. Zhong, J.-Y. Li, Mater. Sci. Eng., B 158 (2009) 69.
[22] L.C. Qin, X. Zhao, K. Hirahara, Y. Miyamoto, Y. Ando, S. Iijima, Nature 408 (2000) 50.
[23] R. Chetty, S. Kundu, W. Xia, M. Brona, W. Schuhmann, V. Chirila, W. Brandl, T. Reinecke, M. Muhler, Electrochim. Acta 54 (2009) 4208.
[24] P.E. Diaz-Flores, F. López-Urías, M. Terrones, J.R. Rangel-Mendez, J. Colloid Interf. Sci. 334 (2009) 124.
[25] D.-P. Kim, C.L. Lim, T. Mihalisin, P. Heiney, M.M. Labes, Chem. Mater. 3 (1991) 686.
[26] K.-Y. Chun, H.S. Lee, C.J. Lee, Carbon 47 (2009) 169.
[27] B. Wang, Y. Ma, Y. Wu, N. Li, Y. Huang, Y. Chen, Carbon 47 (2009) 2112.
[28] V. Krstić, G.L.J.A. Rikken, P. Bernier, S. Roth, M. Glerup, Europhys. Lett. 77 (2007) 37001.
[29] (a) V.G. Pol, S.V. Pol, J.M.C. Moreno, A. Gedanken, Carbon 44 (2006) 3285;
(b) C.P. Ewels, M. Glerup, J. Nanosci. Nanotechnol. 5 (2005) 1345.
[30] T. Cheng, Z. Fang, G. Zou, Q. Hu, B. Hu, X. Yang, Y. ZHANG, Bull. Mater. Sci. 29 (2006) 701.
[31] J. Zhang, J. Li, J. Cao, Y. Qian, Mater. Lett. 62 (2008) 1839.
[32] A.A. Simenel, E.A. Morozova, Y.V. Kuzmenko, L.V. Snegur, J. Organomet. Chem. 665 (2003) 13.
[33] (a) P.T.A. Reilly, W.B. Whitten, Carbon 44 (2006) 1653;
(b) E.G. Wang, Z.G. Guo, J. Ma, M.M. Zhou, Y.K. Pu, S. Liu, G.Y. Zhang, D.Y. Zhong, Carbon 41 (2003) 1827.
[34] (a) T. Watanabe, T. Notoya, T. Ishigaki, H. Kuwano, H. Tanaka, Y. Moriyoshi, Thin Solid Films 506–507 (2006) 263;
(b) Y. Shiratori, H. Hiraoka, M. Yamamoto, Mater. Chem. Phys. 87 (2004) 31.
[35] (a) N. Sano, H. Akazawa, T. Kikuchi, T. Kanki, Carbon 41 (2003) 2159;
(b) W. Wasel, K. Kuwana, P.T.A. Reilly, K. Saito, Carbon 45 (2007) 833.
[36] V.O. Nyamori, E.N. Nxumalo, N.J. Coville, J. Organomet. Chem. 694 (2009) 2222.
[37] R. Andrew, D. Jacque, A. Rao, F. Derbyshire, D. Qian, X. Fan, E. Dickey, J. Chen. Chem. Phys. Lett. 303 (1999) 467.
[38] C. Lee, C. Luy, W. Kin, H. Lee, I. Cho, Chem. Phys. Lett. 359 (2002) 115.
[39] C. Tang, B. Yoshio, D. Golbert, F. Xu, Carbon 42 (2004) 2625.
[40] Y.-Y. Fan, A. Kaufmann, A. Mukasyan, A. Varma, Carbon 14 (2006) 2160.
[41] X.Y. Tao, X.B. Zhang, F.Y. Sun, J.P. Cheng, F. Liu, Z.Q. Luo, Diamond Relat. Mater. 16 (2007) 425.
[42] F. Villalpando-Paez, A. Zamudio, A.L. Elias, H. Son, E.B. Barros, et al., Chem. Phys. Lett. 424 (2006) 345.
[43] S. Maldonado, S. Morin, K.J. Stevenson, Carbon 44 (2006) 1429.
[44] A.M.F. Lima, A.W. Musumeci, H.-W. Liu, E.R. Waclawik, G.G. Silva, J. Therm. Anal. Calorim. 97 (2009) 257.
[45] D. Bom, R. Andrews, D. Jacques, J. Anthony, B. Chen, M.S. Meier, J.P. Selegue, Nano Lett. 2 (2002) 615.
[46] G. Kudashov, V. Okotrub, G. Bulusheva, P. Asanov, V. Shubin, F. Yudanov, L. Yadanova, S. Danilovich, G. Abrosimor, J. Phys. Chem. B 108 (2004) 9048.
[47] F. Villalpando-Paez, A. Zamudio, A.L. Elias, H. Son, E.B. Barros, et al., Chem. Phys. Lett. 424 (2006) 345.
[48] M. Laskoski, T.M. Keller, S.B. Qadri, Carbon 45 (2007) 443.
[49] T.M. Keller, S.B. Qadri, Chem. Mater. 16 (2004) 1091.
[50] J. Kaufman, S. Melin, Phys. Rev. B: Condens. Matter 39 (1989) 13053.